308 Androgen Receptor Expression Is Higher in CK5/6 Negative versus CK5/6 Positive Triple-Negative Breast Cancers

Tao Zuo, Ali Cicek, Olivia L Snir, Yuanxin Liang, Malini Harigopal. Yale School of Medicine, New Haven, CT; Tufts Medical Center, Boston, MA.

Background: Androgen receptor (AR) expression is observed in about 25% to 75% of triple-negative breast cancers (TNBCs). However the degree of AR expression in TNBC varies widely depending on the cancer subtypes, cutoff for positivity and assay methodology.

Design: TMAs with 291 TNBCs of which 228 were available for immunohistochemical study for AR and CK5/6 expression. The percentage and intensity of both markers were evaluated by two pathologists independently.

Results: The Pearson correlation between two pathologists for AR score was R^2=0.94, CK5/6 positive (+) cases (R^2=0.89), and CK5/6 negative (-) cases (R^2=0.9595). AR expression in TNBCs using 1% and 10% cutoff was 41% and 28% respectively of all TNBCs. CK5/6 expression was seen in 122 of 228 (54%), 106 of 228 (46%) TNBCs. Within AR positive TNBCs using 1% cutoff, in CK5/6+ and CK5/6- groups (56 AR+/CK5/6- and 34 AR+/CK5/6+) there was no statistically significant difference (p = 0.207). Within AR positive TNBCs using 10% cutoff, in CK5/6+ and CK5/6- groups (43 AR+/CK5/6- and 20 AR+/CK5/6+) there was statistically significant difference (p= 0.0247). The percentage and intensity of AR expression in CK5/6 negative cases was higher compared with CK5/6 positive cases (p= 0.0036, p= 0.0325) respectively.

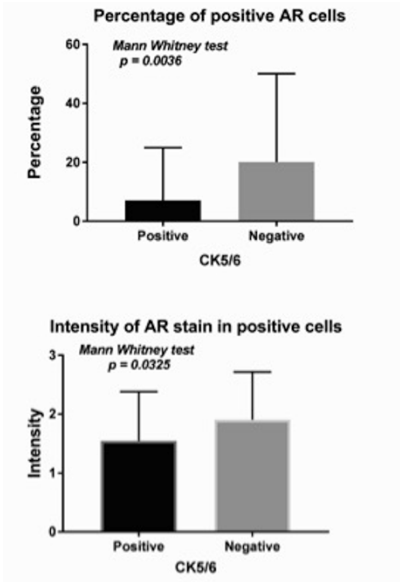

The mean follow-up time in AR+/CK5/6+ was 92 months (mths) (range 24 -180 mths, SD 47.5) versus (vs) a mean follow up time in AR+/CK5/6- of 121 mths (range 48-252 mths, SD 55.2). There was statistically significant difference in survival time for patients with AR+/CK5/6+ TNBCs when compared with AR+/CK5/6- TNBCs (chi square test p value=0.0007).

Conclusions: AR expression is significantly higher in CK5/6- vs CK5/6+ TNBCs. Among AR positive cases, CK5/6- subtype has less favorable outcome compared with CK5/6+.

Cardiovascular Pathology

309 The Role of IgG4 in Acquired Aortic Valve Stenosis: A Study of 110 Consecutive Surgical Resected Aortic Valves

Melanie Bois, Ahmed U Fayyaz, William D Edwards, Joseph J Maleszewski. Mayo Clinic, Rochester, MN.

Background: Mechanisms leading to calcification and fibrosis of aortic valves (AV) are not well understood. Inflammatory and immune processes may contribute to progression of the disease. Anecdotal case reports suggest that immunoglobulin G4 (IgG4)+ plasma cells (PC) may play a role in a subset of degenerative AV disease. No previous study has demonstrated elevated IgG4+ PC in the various types of aortic stenosis.

Design: 110 surgically excised, stenotic AV were consecutively procured. Cases were photographed, measured, decalcified (24-48 hrs), and sampled for histopathologic evaluation. 9 autopsy-derived controls were obtained from individuals without heart disease, hypertension, or an underlying inflammatory condition. Salient clinical and demographic information was abstracted from the medical record. Valves were classified as degenerative, congenitally bicuspid (BAV), or postinflammatory. Immunoglobulin G (IgG) and IgG4 IHC was performed. A single "hot spot" for IgG+ and IgG4+ cells was manually enumerated, and a ratio of IgG4+ to IgG+ cells was calculated.

Results: The cohort (63 men, 47 women) had a mean age of 74 years (range, 47-94). 78 (71%) were classified as degenerative fibrocalcific disease, 22 (20%) as congenitally BAV, and 10 (9%) as postinflammatory.

	Degenerative Fibrocalcific		Congentially Bicuspid		Postinflammatory		Controls (n=9)
	Low IgG4 (n=76)	High IgG4 (n=2)	Low IgG4 (n=19)	High IgG4 (n=3)	Low IgG4 (n=9)	High IgG4 (n=1)	
Age yrs, Mean (range)	77 (53-94)	78.5 (77-80)	67 (47-86)	69 (63-72)	69 (50-80)	74	61 (27-74)
Sex, M (F)	43 (33)	1 (1)	12 (7)	2 (1)	4 (5)	1 (0)	2 (7)
IgG-positive cells, Median (range)	7 (1-150)	38 (24-52)	6 (2-38)	75 (33-141)	13 (1-124)	25	3 (0-11)
IgG4-positive cells, Median (range)	2 (0-15)	16.5 (12-21)	2 (0-8)	61 (17-109)	2 (0-12)	23	0 (0-2)
IgG4:IgG ratio, Median	0.2	0.45	0.21	0.77	0.08	0.92	0

Aortic stenosis was severe in 105 cases and moderate in 5. 27 cases had increased IgG+ cells per high power field (>15), of which 6 showed an IgG4+:IgG+ PC ratio of >0.50 or IgG4+ PC count >20. Of the 6, all had severe stenosis; 3 valves were congenitally BAV, 2 were degenerative, and 1 was postinflammatory. None had clinical features of IgG4-related disease.

Conclusions: This study analyzed stenotic AV for increased IgG4+ PC. A subset of AV (both tricuspid and bicuspid) had increased IgG4+ PC. This finding differs from current literature on the topic and adds to the body of literature published on IgG4-related disease in the AV.

310 The Pathology of Subaortic Membranes: An Analysis of 83 Surgically Resected Cases with Molecular Genetic Correlation

Melanie Bois, Linnea M Baudhuin, Michelle L Kluge, Katrina E Kotzer, Laura J Train, Michael J Ackerman, Joseph J Maleszewski. Mayo Clinic, Rochester, MN.

Background: Subaortic membranes (SAM) are subvalvular collections of fibro(muscular) tissue that result in fixed obstruction. The pathogenesis of subaortic membranes (SAM) remains obscure and while both congenital and acquired forms have been identified, the latter is thought to be more common. Phenotypic overlap exists with other forms of outflow obstruction, such as hypertrophic cardiomyopathy (HCM) and differentiating between them is important given the heritable implications of cardiomyopathic states. Herein, histopathologic and molecular genetic features of a population of 83 surgically resected cases of SAM are evaluated.

Design: Formalin-fixed paraffin embedded (FFPE) tissue was obtained on 83 patients having undergone surgical resection of a discrete or tunnel SAM (2009-2015). Clinical information and hemodynamic data was abstracted from the medical record. Light microscopic features, including myocyte disarray, myocyte hypertrophy, and interstitial fibrosis were semiquantitatively scored. Extracted genomic DNA underwent Agilent SureSelect targeted capture of 54 genes associated with cardiomyopathies, followed by sequencing on the Illumina MiSeq platform. Variants were classified according to established guidelines.

Results: 83 patients (54 women) were included in the study, with a mean age of 49.8 years (range, 4-80). 77 cases of SAM were discrete membranous, while 6 were tunnel-type. Myocyte hypertrophy was absent or mild in 6 cases, moderate in 53 and severe in 23 cases. Interstitial fibrosis was absent or mild in 56 cases, moderate in 25, and severe in 1. Myocyte disarray was absent or mild in 75 cases and moderate in 7. The majority of genetic variants identified were benign polymorphisms; however, 4 pathogenic/likely pathogenic and 77 variants of unknown significance were identified (average, 1.7/case). Of the pathogenic/likely pathogenic variants, mutations in *PTPN11* were present in 2 cases, *MYH7* mutation in 1, and *SOS1* in 1 case. 25 cases were believed clinically to have concomitant HCM, though none of those carried a molecular genetic mutation compatible with such. No histopathologic or clinical parameter appeared to correlate with identified pathogenic mutations.

Conclusions: Hitherto, this is the first systematic survey of SAMs to evaluate their histopathologic features. Additionally, it is the largest series of cases of SAMs to undergo molecular genetic interrogation to evaluate for concomitant cardiomyopathy or syndrome. Histologic findings alone did not appear to be a predictor of underlying genetic variation to help in evaluation for a cardiomyopathic or syndromic state.

311 Arrhythmogenic Cardiomyopathy: A Genotype-Phenotype Correlation of 15 Cases

Melanie Bois, Michelle L Kluge, Katrina E Kotzer, Laura J Train, Joseph J Maleszewski. Mayo Clinic, Rochester, MN.

Background: Arrhythmogenic cardiomyopathy (AC) is a rare and potential fatal form of heritable cardiovascular disease. Despite important advances in understanding the genetic basis of AC, identification of novel potentially pathogenic mutations remains paramount in the recognition, diagnosis and treatment of at-risk patients. Herein, genetic analysis of 15 AC specimens was performed and correlated with gross and histopathologic features.

Design: Formalin-fixed paraffin embedded tissue was obtained on 15 archived AC cases (2009-2015), meeting established clinical diagnostic criteria for said diagnosis. Clinical information was abstracted from the medical record. Gross and histopathologic features of AC cases were recorded. Extracted genomic DNA underwent Agilent SureSelect targeted capture of 54 genes associated with cardiomyopathies, followed by sequencing on the Illumina MiSeq. Variants were classified according to established American College of Medial Genetics (ACMG) guidelines.

Results: 15 patients (8 men) with a mean age of 48 years (range, 11-69) were included in the study (12 explant; 3 autopsy). 9 patients had right-ventricular (RV) involvement,

while 3 had left ventricular (LV) or biventricular (biV) involvement, respectively. Involvement was characterized by transmural fatty or fibrofatty replacement of the ventricular myocardium. 4 cases exhibited significant biventricular dilatation. Of identified genetic variants, 4 pathogenic (P) or likely pathogenic (LP) mutations were identified (2 each) and 10 variants of unknown significance were documented (average of 1.1 variants/case). 2 *PKP2* mutations (1 P, 1 LP) were associated with RV disease. 1 RV case showed a pathogenic *MYH7* mutation, a gene generally observed in patients with hypertrophic or dilated cardiomyopathy (CM). This patient had near-transmural fatty replacement of the RV, biV dilatation, and no asymmetrical LV hypertrophy. An additional LP variant in *JUP* was observed and associated with LV disease. None of the cases with significant dilatation were associated with P or LP variants. No pathologic features appeared predictive of pathogenic mutations.

Conclusions: The discovery of a pathogenic *MYH7* mutation in a phenotypic AC case provides novel insights into the phenotypic heterogeneity of cardiomyopathies and the genetic overlap that may exist between them. No gross or histopathologic parameter appeared to be associated with the presence or type of molecular genetic alteration identified. This survey also expands the database of variants identified in cases of phenoytype-positive AC.

312 S100a1 Levels Predict Cardiac Functional Recovery After LVAD Implantation

Baidarbhi Chakraborty, Eman Hamad, Theodore Vasiliadis, Rachana Choksi, Shiguang Liu, Linda Mamone, Nirag Jhala, He Wang. Temple University Hospital, Philadelphia, PA.

Background: S100A1 is a key regulator of calcium (Ca^{2+}) cycling in cardiomyocytes. S100A1 gene transfer prevents and reverses HF (Heart Failure) in mouse, rat and pig models. Very limited data are available regarding S100A1 in failing human hearts, especially after left ventricular assisted device (LVAD) implantation. We have previously shown implantation of LVAD improves functions of failing hearts. Here we hypothesize that changes of S100A1 levels before and after LVAD implantation is a reliable predictor of cardiac function recovery.

Design: Thirteen pairs of failing human cardiac tissues were collected (before LVAD and pre-explant) from the cardiac tissue bank in Temple University Hospital, including 2 females and 11 males with average age of 57 years. Primary etiology for cardiac failure were ischemic cardiomyopathy (n=6) and nonischemic cardiomyopathy (n=7).The duration of LVAD ranged from 1.5 to 56 months (average: 10 months). Hemodynamic data and Echo measurements before LVAD implant were compared to measurements pre-explant. Rapid tissue procurement in the operating room was performed within 2 hours of cardioplegic arrest. S100A1mRNA expression was analyzed on frozen left ventricular tissue utilizing quantitative Reverse transcription polymerase chain reaction (qRT-PCR). Tissues for light microscopy and immunohistochemistry were fixed in 10% neutralized formalin. Cardiac apoptosis were measured by immunostain of caspase-3.

Results: Our results demonstrate that S100A1 mRNA levels positively correlated with cardiac index (CI, r= 0.54, p=0.04) and left ventricular end-diastolic diameter (LCIDd, r =0.47, p=0.03, n=13). Similar correlations were noted between S100A1 protein expression (by immunohistochemistry) and cardiac functional indices. Furthermore, we also noted that pre-LVAD explant S100A1 protein expression level inversely correlated with left ventricular apoptosis at time of LVAD explantation (r=0.6, p=0.02).

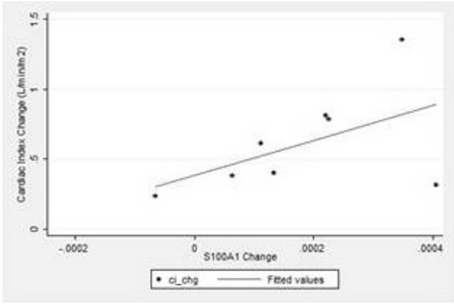

Conclusions: We conclude that changes of S100A1 expression levels before LVAD implant and pre-explant correlate well with cardiac functional recovery after LVAD implant. Further, S100A1 level after LVAD implantation correlated with decreased apoptosis of cardiomyocytes in failing human hearts.

313 Small Vessel and Soft Tissue Histology in End-Stage Renal Disease: Specificity of Diagnostic Criteria for Calciphylaxis

Carla Ellis, William C O'Neill. Emory University, Atlanta, Georgia; Emory University, Atlanta, GA.

Background: Calciphylaxis is a rare disease characterized by skin ulceration and tissue necrosis presumably resulting from vascular calcification that typically occurs in the setting of end-stage renal disease (ESRD). Histologic criteria variably include intimal hypertrophy, medial calcification and/or thrombosis of small arteries, and extravascular (soft tissue) calcification, but the specificity of each is unknown.

Design: 26 amputations from above (11) and below (15) the knee in 21 ESRD patients with peripheral arterial disease (PAD) were identified from pathology records for 2014-2015. Sections from the viable margins were retrieved and both hematoxylin and eosin (H&E) and Von Kossa stains were prepared and reviewed by a single pathologist. Chart review was performed by a single nephrologist. None of the amputation patients had a clinical presentation suggestive of calciphylaxis. As controls, 18 skin biopsies performed for a clinical suspicion of calciphylaxis were retrospectively reviewed.

Results: The average age was 63.7 years (range 43-83). (76%) were male, (67%) were diabetics. In the amputation sections, bulky, large vessel calcifications were identified in 24/26 (92%) of specimens, consistent with PAD. However, 8/26 (31%) also showed dermal/epidermal arteriolar (small vessel) calcification, and 11/26 (42%) showed extravascular soft tissue calcification. Intimal hyperplasia and small vessel thromboses were observed in 3 and 4 cases respectively (12% and 15%). Von Kossa staining in the amupation specimens, revealed vascular calcification in small vessels that had not been identified by H and E. In the skin biopsy sections, Von Kossa (or any other stain for the detection of calcium) stains had not been performed (0/18 cases). The skin biopsies revealed histopathologic findings that varied from definitive for (22%), negative for (28%), equivocal (33%), and compatible with (17%) calciphylaxis.

Conclusions: Histopathologic findings historically associated with calciphylaxis on skin biopsies can also be seen in liberally sampled and viable tissue from unaffected ESRD patients. While the results are not necessarily applicable to patients without PAD, they do indicate that there is considerable histopathologic overlap (despite divergent clinical presentations) among both entities. These data call into question the specificity of the histologic diagnosis of calciphylaxis, particularly when the diagnosis is only definitively made 22% of the time in the proper clinical context.

314 Thrombus on the Inflow Cannula of the HeartWare HVAD: An Update

Carolyn H Glass, Gregory A Fishbein, Kyle C Strickland, Jaclyn C Watkins, Robert Padera. Brigham and Women's Hospital, Boston, MA; David Geffen School of Medicine, UCLA, Los Angeles, CA.

Background: The HeartWare HVAD (HeartWare, Inc, Framingham, MA) is a continuous-flow left ventricular assist device (LVAD) approved by the FDA in 2012 as a bridge to transplant in patients with end-stage left ventricular heart failure. The current inflow cannula has a smooth outer surface near the inflow edge and a sintered collar of titanium microspheres near the pump. A previous case series of HeartWare patients bridged to transplant revealed thrombus on the outer surface of the inflow cannula in 8/8 patients, predominantly at the smooth-sintered interface, associated with a clinical stroke rate of 12.5%.

Design: Cases of HVAD devices removed at the time of heart transplant were identified in the surgical pathology database. The gross and microscopic findings were reviewed along with clinical data.

Results: A total of 18 patients (15 men and 3 women, mean age 47) with 20 HVAD implants (mean support time 309 days, range 71 to 608) with dilated cardiomyopathy (13 patients), ischemic heart disease (2 patients), hypertrophic cardiomyopathy (1 patient), congenital valvular disease (1 patient) and lymphocytic myocarditis (1 patient) were included. Two patients had HVADs in the left ventricle and in the right atrium to provide biventricular support. All patients received post-implantation anti-coagulation with an INR goal of 2 to 3. Gross pathologic examination revealed thrombi on the outer aspect of the HVAD inflow cannula (thrombus size 0.4 cm to 4.5 cm, mean 1.6 cm) in 19 of 20 devices (95%). The inflow cannula of the one device that did not develop thrombus was positioned such that the smooth-sintered interface was buried in the ventricular myocardium and not in contact with blood in the ventricular chamber. Complications during the period of device support included 8 thromboembolic events (44%) including 6 strokes (33%), 1 splenic infarct, and 1 intracoronary thromboembolus. Patients suffered strokes 4 to 174 days (mean 82) after HVAD placement and had thrombi ranging from 0.4 to 2.5 cm (mean 1.1 cm). Histological evaluation of these thrombi revealed bland organized thrombus without evidence of infection.

Conclusions: We report here an extension of the original study to a total of 18 patients with 20 HVAD implants who were all successfully bridged to transplant. We validate the near-universal formation of thrombus around the HeartWare HVAD inflow cannula associated with a clinical thromboembolic event in almost half the patients, the majority of which were strokes. The nidus for thrombus formation appears to be the smooth-sintered interface.

315 Characterizing the Histopathology of Immune Checkpoint Inhibitor Blockade Induced Myocarditis

Carolyn H Glass, Richard N Mitchell, Robert Padera, Javid Moslehi, Andrew H Lichtman. Brigham and Women's Hospital, Boston, MA; Vanderbilt University Medical Center, Nashville, TN.

Background: Immune checkpoint inhibitor blockade (ICIB) is increasingly used as an effective therapy in cancer management. Several immune related adverse effects (irAEs) have been described. Although myocarditis is a rare irAE, the incidence and severity of this complication is unknown. We report here a series of ICIB induced myocarditis cases, and histologically characterize the spectrum of disease.

Design: Material from 8 autopsies on cancer patients treated with various chemotherapy and ICIB regimens from December 2014 to June 2016 was reviewed. Three additional cases of presumed ICIB induced myocarditis (1 endomyocardial biopsy, 2 outside hospital autopsies) were examined, yielding 4 ICIB myocarditis cases.

Results: Focal lymphocytic myocarditis was identified in 1 of 8 (incidence 12.5%) ICIB treated, in-house autopsy cases. For the additional 3 ICIB myocarditis patients, 2 experienced new complete heart block and 1 patient had severe heart failure. Histological findings showed fulminant myocarditis 12 to 30 (mean 19) days post treatment. Only 1 patient improved with aggressive steroid treatment, while 2 patients died within 2 weeks after presentation. ICIB myocarditis patients (3 men, 1 woman, mean age 57) received treatment for mean of 59 days. Histologic and immunohistochemical (IHC) evaluation showed a distinct pattern in ICIB induced myocarditis. Compared with idiopathic lymphocytic myocarditis and transplant rejection case controls, 3 of 4 ICIB myocarditis patients exhibited extensive multifocal coagulative necrosis. There was also strong programmed death ligand-1 (PD-L1) expression on myocytes and endothelial cells in areas of lymphocytic infiltration. In contrast, there was minimal coagulation necrosis,

and minimal PD-L1 expression in myocytes in focal ICIB myocarditis. Interestingly, there was complete absence of PD-L1 expression in lymphocytes and myocytes in idiopathic fulminant lymphocytic myocarditis and ISHLT Grade 2 transplant rejection control hearts. IHC for HLA-DR, a surrogate for IFN-gamma production, was diffusely positive in all the ICIB myocarditis cases, consistent with previously reported murine models of PD-L1 inhibition induced myocarditis.

Conclusions: In summary, ICIB myocarditis may be more common than previously reported, and can potentially have fatal complications with distinct histopathological features. Biomarkers of myocyte injury may be indicated to provide early detection, and allow therapeutic intervention.

316 PSEN1 as an Adjunct for Diagnosis of Human Myocarditis

Paul J Hanson, Erika L Jang, Harpreet Rai, Angela Y Chang, Angela Y Mo, Bruce M McManus, Michael A Seidman. University of British Columbia, Vancouver, BC, Canada; Providence Health Care, Vancouver, BC, Canada.

Background: Myocarditis, defined as inflammation of the heart muscle, is a spectrum of conditions causing considerable morbidity and mortality, resulting from various etiologies, including infection, autoimmunity, or chemical exposure. As such, diagnosing myocarditis can be quite difficult and determining etiology even more so. The gold standard of diagnosis is endomyocardial biopsy showing inflammation with or without myocyte damage in the absence of an ischemic event. However, due to the spatial and structural heterogeneity of myocarditis, diagnostic sensitivity is estimated as low as 30%. To improve upon this, we examined several markers implicated in the pathogenesis of viral myocarditis in animal models as possible diagnostic adjuncts. PSEN1 (the gene encoding presenilin 1) emerged as a promising candidate. This study aims to formally evaluate PSEN1 as a diagnostic adjunct.

Design: Forty six (46) cases were examined for PSEN1 staining (20 lymphocytic active or healing myocarditis, 4 eosinophilic myocarditis, 4 idiopathic dilated cardiomyopathy, 4 hypertrophic cardiomyopathy, 4 sarcoidosis, 3 transplant rejection, 1 Lyme disease, 1 toxoplasmosis, and 5 normal controls). All cases were obtained from the Cardiovascular Tissue Registry in the Centre for Heart Lung Innovation, under approved human ethics protocols. Levels of PSEN1 were evaluated using colour segmentation and scoring conducted by three individual subspecialty cardiac pathologists blinded to diagnosis. Statistical analysis was performed using Mann Whitney *U* test and receiver operating characteristics (ROC) curves.

Results: Colour segmentation and pathologist scoring correlated with each other well (Spearman's *rho* correlation coefficient 0.71 or better in all comparisons). PSEN1 is expressed at significantly higher levels in lymphocytic myocarditis cases as compared to normals and to all other pathologies (all *p*-values less than 0.005). The ROC curves for diagnosing myocarditis as compared to other pathologies using PSEN1 staining have areas under the curve (AUCs, or c-statistics) ranging from 0.78 to 0.88. Of note, several "false positive" cases were those with idiopathic dilated cardiomyopathy, such cardiomyopathy reflects the end stage of a prior lymphocytic myocarditis. Case subset analyses and validation on biopsy specimens are under way.

Conclusions: PSEN1 immunohistochemistry appears to be a helpful diagnostic adjunct for identifying myocarditis, even in minimally inflamed specimens and in tissue obtained long after the initial insult.

317 Xenoimmune Response Can Elicit Early Postoperative Bioprothetic Valve Degeneration

Kishio Kuroda, Kenji Kuwaki, Kenta Uto, Saeko Yoshizawa, Takuo Hayashi, Toshio Nishikawa, Atsushi Amano, Takashi Yao. Juntendo University, Tokyo, Japan; Juntedo University, Tokyo, Japan; Tokyo Women's medical university, Tokyo, Japan.

Background: Bioprosthetic heart valves (BHV) have been widely used in elderly patients and those ineligible for anticoagulation therapy. However, it is recognized that there are a certain number of patients developing valvular malfunction during the early post-operative period following valvular replacement surgery using BHV.

Design: Pathological evaluation including immnohistological staining of inflammatory cells as well as α-Gal (galactose-alpha-1,3-galactase) was performed in the following valves; (i) unused porcine and bovine BHVs (glutaraldehyde-fixed) provided from the manufacturer (n=1 each), (ii) BHVs obtained at the time of 2nd valvular replacement surgery performed within a mean of 5 years from the 1st surgery (n=5), (iii) homografts obtained at the time of 2nd valuvular surgery after 20 years from the initial surgery (n=2). Untreated porcine heart valve tissue was used as a positive control for α-Gal.

Results: Unused fixed valves were still positive for a-Gal. In BHVs which had developed valvular dysfunction, strong expression of a-Gal associated with remarkable cell proliferation was observed along with positive CD68 (macrophages) and CD 3 (activated T cells), which were not seen in calcified tissues. The L26 showed weak positivity. On the other hand, resected homografts showed calcification of the degenerated leaflets without remarkable cell proliferation but a weak CD68 positivity.

Conclusions: BHV have been considered to be free from xeno-immunogeneity by glutaraldehyde-fixation. However, a possible residual immunogeneity, revealed by a-Gal positivity found in the unused valves, might advocate xenoimmune response of the human immunity against the valve. Our findings suggest the bioprosthetic valve degeneration may be the result of xenograft rejection, which could be prevented by immunosuppressive therapy in selected population.

318 Molecular Genetics of Left Ventricular Noncompaction Cardiomyopathy

Vidhya Nair, Linda Kocovski, Guillaume Paré. McMaster University, Hamilton, ON, Canada.

Background: Left ventricular noncompaction (LVNC) is a recently defined cardiomyopathy characterized by a pattern of prominent trabecular meshwork and deep intertrabecular recesses. It is believed to be due to an arrest of normal endomyocardial morphogenesis. There are numerous genes implicated in the pathogenesis. Individuals with the condition may be asymptomatic or may suffer a variety of sequelae including left ventricular systolic dysfunction, arrhythmias, thromboembolic events, heart failure, and sudden death secondary to lethal ventricular arrhythmias. Our objective was to determine the molecular abnormalities leading to LVNC in postmortem cases with gross and microscopic pathologic features consistent with the condition.

Design: Four unrelated postmortem cases with morphologic and histologic diagnoses of LVNC were identified: a 26-year-old male, a 15-month-old female, a 5-month-old female, and a 10-day-old female, who all died unexpectedly. Consent was obtained to extract DNA from two of the cases (snap frozen myocardial tissue from the 26-year-old male, and formalin fixed paraffin embedded myocardial tissue and snap frozen renal tissue from the 5-month-old female). The samples were subjected to sequence capture using Agilent SureSelect and underwent subsequent high coverage sequencing using Ion Proton System for Next-Generation Sequencing (Life Technologies). Candidate mutations were determined based upon pathogenicity prediction scores and were cross-referenced with known genes associated with LVNC from various databases.

Results: Eight candidate genes known to be involved with cardiac function or in the pathogenesis of cardiomyopathy were detected from the first case (26-year-old male). Three of these genes (ARHGEF25, NOTCH1, TTN) have been implicated in either the pathogenesis of LVNC or in the exacerbation of the LVNC phenotype. Two candidate genes were detected from the second case (5-month-old female) that were known to be associated with cardiac defects or cardiomyopathy (CSRP3, NOTCH2). Neither of those genes, however, was known to be associated with LVNC in particular, based upon published data at the time.

Conclusions: Determining the underlying causative genetic abnormalities of LVNC will improve our knowledge of the pathogenesis and inheritance patterns of LVNC. This will allow for future targeted genetic testing of family members and for the institution of preventive measures.

319 Assessment of the ISHLT Antibody-Mediated Rejection Grading System for Cardiac Transplantation and Association with Donor Specific Antibodies and Endothelial Activation

Aivi Nguyen, Stephanie Dean, Renee Frank, Maria Molina, Malek Kamoun, Priti Lal. Hospital of the University of Pennsylvania, Philadelphia, PA.

Background: Antibody-mediated rejection (AMR) is a diagnostic and therapeutic challenge in heart transplantation. The International Society for Heart and Lung Transplant (ISHLT) proposed a new grading scheme for AMR in 2011 that combines both histopathologic and immunologic features.

Design: This retrospective, single institutional analysis (2005-2011) evaluated cardiac transplant endomyocardial biopsies (EMBs) of patients who had concurrent C4d immunofluorescence (IF) and donor specific antibody (DSA) levels. After blinded screening and categorization of EMBs for the histopathologic AMR features, EMBs were then immunostained with E-selectin, a purported marker for endothelial activation. EMBs with >2 or >4 histopathologic features were considered at least AMR1 or AMR3, respectively. C4d IF was deemed positive if >50% capillary staining was observed. E-selectin was positive if membranous endothelial staining was present.

Results: AMR was assessed in 106 EMBs and further classified as follows:

AMR Grade	Number	DSA	Positive IF	Positive E-selectin
AMR0	38	12	0	1
AMR1-h	48	21	0	3
AMR1-i	3	2	3	0
AMR2	13	13	13	3
AMR3	4	3	1	0
	106	51	17	7

Circulating DSA was observed in 48% of patients spanning all grades (AMR0 to AMR3). Endothelial activation was the most frequently observed histologic finding across all AMR grades (68%) with a 78% sensitivity in predicting a positive DSA status. Moreover, endothelial activation and intravascular macrophages independently correlated with DSA status ($p<0.01$). Among the pAMR+ specimens, E-selectin immunohistochemistry was overall positive in only 10%, and predominantly in AMR1-h and AMR-2. All E-selectin positive cases histologically correlated with endothelial activation and interstitial edema. Lastly, of the E-selectin positive cases, 40% were concomitantly C4d positive at the time of biopsy. Interestingly, all cases with E-selectin positivity went on to develop C4d positivity.

Conclusions: The ISHLT 2011 pAMR grading system statistically correlates with DSA. Moreover, the presence of endothelial activation should raise the suspicion for AMR. This study's proposed immunomarker for endothelial activation, E-selectin, was biologically promising, though the proportion of cases staining positive may be too small for clinical significance and will be further characterized.

320 Cardiac Iron Overload Following Liver Transplantation in Patients without Hemochromatosis

Stavroula Papadodima, Ricard Masia, James R Stone. National and Kapodistrian University of Athens, Athens, Greece; Massachusetts General Hospital, Harvard Medical School, Boston, MA.

Background: Cardiac iron overload following liver transplantation in patients without hemochromatosis has been reported to result in heart failure and/or death in case reports and small case series. However, the frequency and causes of cardiac iron overload following liver transplantation and its relationship to cardiac dysfunction overall in this setting are unclear. This study examined the presence of cardiac iron overlaod in patients who underwent cardiac transplantation or autopsy within 1 year of liver transplantation.

Design: The primary inclusion criteria for this study were liver transplantation between 2000-2016, followed by autopsy or cardiac transplantation within 1 year. Cases of known hemochromatosis were excluded. Iron stains were performed on left ventricular myocardium from either the autopsy or surgical explant, as well as the surgically explanted liver. Laboratory values, transfusion history, and echocardiographic evidence of left ventricular dysfunction were obtained from the medical records.

Results: 19 cases met the study criteria: 18 autopsies and 1 case of cardiac transplantation. Myocardial iron deposition was identified in 7 (37%) of the cases. Post-liver transplant echocardiography was performed on 13 of the 19 patients. New reduced left ventricular ejection fraction (<50%) following liver transplantation occurred in 4 of 5 patients with myocardial iron deposition, compared with 0 of 8 patients without myocardial iron deposition (P=0.007). The presence of myocardial iron deposition was not significantly associated with age, gender, year of liver transplant, post-liver transplant time interval, presence of cirrhosis or hepatitis C, or the pre-liver transplant serum iron or ferritin levels. However, in the patients with myocardial iron deposition, there was a trend toward higher pre-transplant transferrin saturation (median 100% vs 69%, P=0.13) and more units of red blood cells (RBCs) transfused (median 72 units vs 21 units, P=0.035). The product of the transferrin saturation multiplied by the number of units of RBCs transfused was significantly greater in the patients with myocardial iron deposition [4,700 (3,100-9,800) vs 680 (400-2,300), median (interquartile range), P=0.003].

Conclusions: Cardiac iron overload is frequently associated with cardiac dysfunction following liver transplantation and is related to the pre-liver transplant transferrin saturation and the amount of RBCs transfused during and following the surgery.

321 Sudden Coronary Death in the Young: Evidence of a Contractile Phenotype of Smooth Muscle Cells in the Atherosclerotic Plaque

Stefania Rizzo, Matteo Coen, Antonija Sakic, Gaetano Thiene, Giulio Gabbiani, Cristina Basso, Marie-Luce Bochaton-Piallat. University of Padua, Padova, Italy; University of Geneva, Geneva, Switzerland.

Background: Atherosclerotic coronary artery disease precipitating sudden cardiac death (SCD) in the young is peculiar in terms of
extent, site and morphology (mostly fibrocellular due to smooth muscle cells [SMC] proliferation) of the atherosclerotic plaque (AP), usually not complicated by thrombosis. To characterize the SMCs phenotype in coronary AP from young SCD victims.

Design: Among 650 young (<40 years old) victims in the SCD Registry of Northeast Italy, 125 (19%) were due to coronary
atherosclerosis. Sixteen AP from 14 young atherosclerotic SCD victims (all males, age range 19-40 years old) with critical stenosis were selected. Eleven AP from older (>40 years old) atherosclerotic SCD victims (n=10, 9 males)
and normal coronary segments from young people (n=6, 4 males) were used for comparison. To characterize the SMC phenotype, the expression of α-smooth muscle actin (α-SMA), smooth muscle myosin heavy chains (SMMHCs) and caldesmon (CaD) was assessed by immunohistochemistry and morphometric quantification.

Results: The 16 AP from young SCD victims showed a preserved tunica media and abundant α-SMA+ SMCs, significantly higher compared to older SCD victims (α-SMA+ area staining/intima area: 38.82% vs 20.36%, p=0.0005). Moreover, intimal SMCs co-expressed the contractile phenotype markers SMMHCs (11.76% vs 4.34%, p=0.0002) and CaD (9.56% vs 2.39%, p=0.0001).

Conclusions: AP in young SCD victims show abundant SMCs with a contractile phenotype (α-SMA+, SMMHC+ and CaD+). In the setting of critical stenosis, intimal SMC contractility, together with vasospasm due to a preserved tunica media, might contribute to transient coronary occlusion with myocardial ischemia precipitating SCD.

322 Atherosclerotic Plaque Instability in Juvenile Sudden Coronary Death

Stefania Rizzo, Gaetano Thiene, Cristina Basso. Cardiovascular Pathology, Padova, Italy.

Background: The vulnerable atherosclerotic plaque underlying acute coronary syndrome including sudden death (SD) is typically represented by thin-cap fibroatheroma (FA) at risk of rupture and acute thrombosis. However in the young the culprit coronary lesion typically shows a thick fibrous cap, with a small or even absent lipid core (fibrocellular –FC- plaque), and thrombosis when occurring is mostly due to plaque erosion.

Design: The aim of the present study was to assess the prevalence of atherosclerotic coronary artery disease (CAD) and the substrate of plaque instability in young people (≤40 yrs) who died suddenly in the prospective Registry of SD, NorthEast of Italy.
Serial sections investigation of all major epicardial coronary arteries and myocardium was performed and slides routinely processed with H&E and Heidenhain trichrome, according to the Guidelines for SD investigation of the AECVP.

Results: Among a consecutive series of 690 consecutive cases of SD in the young collected in Northeast of Italy, time interval 1980-2016, 125 (18%) were due to atherosclerotic CAD (mean 32.3±5.3, M/F=111/14). In young SD victims, a multivessel CAD was detected in 62 (49%, mean age 34.4±4.5 vs 30.9±5 single vessel disease). A fibrous scar in the myocardium was found only in 34 cases (27%). Acute coronary thrombosis was detected in 49 cases (39%, mean age 33.3±4.1 vs. 31.9±5.7 of those without thrombosis), as a consequence of either plaque erosion in 26 (53%, mean age 31.5±4.3) or rupture in 23 (47%, mean age 35.3±3.8). Erosion occurred upon FC plaques in the majority of cases (15,73%), while rupture typically occurred in FA plaques (100%) (all p <0.01). Among the 76 SD cases without thrombosis (61% of cases), 45 had thick fibrous cap FA (62%) and 29 (38%) FC plaques with critical luminal stenosis, all exhibiting a preserved tunica media and abundant smooth muscle cells proliferation.

Conclusions: Plaque instability in the young may be either "structural", with thrombosis mostly due to erosion, or "functional", due to superimposed vasospasm with vessel hyper-reactivity. Acute ischemia is the usual mechanism of electrical instability, while postinfarction scar is observed in only one fourth of cases. Nearly two thirds of atherosclerotic coronary SD under the age of 40 years are due to either FC or thick cap FA plaques, not complicated by thrombosis. Most of cases present a single vessel disease with exhuberant intimal fibrocellular proliferation devoid of lipids in the setting of smooth muscle cells proliferation and preserved tunica media (so-called premature accelerated atherosclerosis).

323 Early Aortic Valve Pathology as a Precursor to Clinical Stenosis

Maria E Romero, Elena R Ladich, Sho Torii, Robert Kutys, James Atkinson, Frank Kolodgie, Renu Virmani. CVPath Institute, Gaithersburg, MD; Vanderbild University Medical Center, Nashville, TN.

Background: Aortic valvular stenosis is a disease with a long latent period followed by rapid progression to death after the onset of symptoms where the reported average survival is 2 to 5 years. The underlying pathogenesis remains poorly understood, although end-stage dysfunction is complicated by extensive calcification. The aim of this study was to evaluate morphologic features of early aortic valve disease with assessment of inflammatory cells and candidate proteins that are involved in the pathophysiology of early valvular calcification.

Design: Grossly normal AV leaflets (n=34) from 18 autopsied hearts (mean age 61 years) and 8 heavily calcified surgical aortic valve explants (n=24 leaflets) were examined. These were assessed on H&E, Movat pentachrome, PAS, picrosirius red, and von Kossa (calcium) stains. Immunohistochemical markers for inflammatory cells (CD68, CD45RO), interstitial cell phenotypes (a-SMA, desmin, and vimentin) and mineralization (bone morphogenic protein-2 [BMP-2], matrix GLa protein [MGP], and osteoprotegerin [OPG]) were all graded semi-quantitatively. Normal AV leaflets evaluated between age groups by leaflet layer showed statistically significant increase in leaflet thickness at the base, and this increase is directly proportional with age (P value 0.0129).

Results: 23 lesion sites were found in leaflets from autopsy where 5 showed only lipid deposits while 18 had both lipid and calcification. Lesions were exclusively found at the site of valve attachment (44%) and/or region proximal to the line of closure (24%). Speckled calcification (particles ≤2 μm) was indentified in 7 lesions whereas 11 had larger particle size. The lesion morphologies were classified as early (proteoglycan + lipid) or late lipid insudation (lipid only) where significant differences were noted for free cholesterol, calcification and associated proteins MGP and OPG (see graph) while all surgical valves showed extensive calcification with inflammatory cells, fibrin, and varying degrees of bone forming proteins.

Conclusions: Lipid insudation of the valve interstitium is the earliest event followed by speckled calcification with minimal inflammation. The accumulation of free cholesterol is accompanied by larger calcified particulate with expression of mineralization markers, consistent with lesion progression. These results raise the possibility of instituting lipid-lowering therapy early for patients at high risk of developing AS.

324 CD10 Expression in Endothelial Cells of Intramuscular Angioma/Vascular Malformation

Toyohiro Tada, Katsutoshi Miura. Toyokawa City Hospital, Toyokawa, Japan; Hamamatsu University School of Medicine, Hamamatsu, Japan.

Background: Some benign vascular tumors (or tumor-like lesions) (BVTs) are not so easy to classify appropriately by conventional histology; e.g. whether reaction, neoplasm, or malformation. Therefore, useful immunohistochemical markers are required to differentiate each. "Intramuscular angioma (IA)" is defined as a proliferation of benign vascular channels within skeletal muscle (WHO, 2012), but this lesion is considered to be "arteriovenous /vascular malformation" in nature. Recently we noticed that endothelial cells of angiomatous vessels of IA were immunohistochemically CD10-positive. The aim of this study is to examine pathological significance of CD10 expression in IA, and investigate its usefulness for an accurate diagnosis of BVT.

Design: 25 cases of IA were stained immunohistochemically with CD10, and endothelial markers such as CD31, CD34, and podoplanin (D2-40), GLUT1, ERG, and Prox1. Normal tissues (10 cases) with various sized vascular vessels, and other BVTs including cavernous hemangiomas (venous malformations) (5 cases), lobular capillary hemangiomas (pyogenic granulomas, 10 cases), cherry angiomas (5 cases), and lymphangiomas (3 cases) were examined as well.

Results: In 21 cases (84%) of IA, endothelial cells of abnormal vessels expressed CD10 diffusely or focally in cytoplasmic staining pattern. CD31, CD34, podoplanin, ERG, and Prox1 were variously positive depending on the lesion. In cavernous hemangiomas and lymphangiomas, CD10 showed diffuse positivity in endothelial cells in all cases. CD10-poitive vessels were not found in lobular capillary hemangiomas and cherry angiomas. In normal tissues, CD10-positive endothelial cells were not seen in 8 tissues, but found faintly in very small part in two tissues.

Conclusions: CD10-positivity in endothelial cells is a useful marker for histological diagnosis of IH and other vascular malformations, and makes possible to differentiate vascular malformation from other BVTs. However, the etiological significance of CD10 expression in these vascular malformations remains to be studied in future.

325 Increased Histopathology in Marfan Syndrome Compared to Loeys-Dietz Syndrome and Non-Syndromic Aortas

Kevin Waters, Andrew Guajardo, Marc Halushka. Johns Hopkins University SOM, Baltimore, MD.

Background: In 2016, the Society for Cardiovascular Pathology (SCVP) and the Association for European Cardiovascular Pathology (AECVP) developed a new set of nomenclature and definitions for histopathology of the ascending aorta. We specifically investigated Marfan Syndrome (MS), Loeys-Dietz Syndrome (LDS) and non-syndromic aortas to see how our understanding of these diseases is impacted by these new criteria.

Design: Aortic specimens from patients with MS (n=39), LDS (n=21), and non-syndromic patients (n=53) were selected from our surgical archives along with basic phenotypic information. Each case was independently scored by 2+ observers in a blinded fashion for 13 features using H&E and Movat stained slides. Disagreements were adjudicated by a cardiovascular pathologist. All data was categorized, converted into numbers, tabulated, and analyzed using a Mann Whitney U test.

Results: The average age of resection was lower in both MS (30±14) and LDS (20±16) cases than in non-syndromic cases (63±15), but no differences were noted in the sex/racial distribution of the groups. The total medial degeneration score was higher in MS cases (2.2±0.8 in a 0-3 scale) than in LDS cases (1.7±1, $p=4.4x10^{-2}$) or non-syndromic cases (1.7±0.8, $p=2.6x10^{-3}$). Among patients with MS, the average score for mucoid extracellular matrix accumulation (MEMA) was higher for both extent (3.4±1.7 in a 0-6 scale) and severity (3.2±1.9) than that seen in non-syndromic cases (2.4±1.9 $p=3.6x10^{-3}$ and 2.2±1.9 $p=3.7x10^{-3}$; respectively). The average score was not significantly different in patients from non-syndromic cases or from LDS patients for either extent (2.6±1.8) or severity (2.4±1.8). Average elastic fiber loss was pronounced for both extent and severity in both MS (2.2±0.9 and 2.2±1, respectively; 0-3 scale) and LDS (1.7±1.1 and 1.7±1.2) compared to non-syndromic cases (1.0±1.2 and 0.9±1.1; all p values < 0.02). Conversely, the average extent and severity of smooth muscle cell nuclei loss was greater in non-syndromic cases (1.8±1.0 and 1.4±0.7) compared to MS (0.6±0.9 and 0.6±0.8) and LDS (0.5±0.9 and 0.3±0.6; all p values $<10^{-4}$).

Conclusions: This is the first evaluation of the new AECVP/SCVP aorta nomenclature and definitions in MS and LDS aortas. We clearly demonstrate that, in general, MS has more significant medial degeneration at the time of surgery compared to LDS or non-syndromic cases. There is also significantly more elastic fiber loss and less smooth muscle cell loss in these syndromic diseases compared to non-syndromic diseases.

326 Sudden Death in Hypertrophic Cardiomyopathy. Data from a Large Pathology Registry

Joseph Westaby, Mary N Sheppard. St George's University of London, London, United Kingdom.

Background: Hypertrophic cardiomyopathy (HCM) is reported as a common cause of sudden cardiac death (SCD) in young people. Exercise is considered a trigger to fatal arrhythmias and International recommendations advise to avoid competitive sports in individuals with HCM. It is unclear however if SCD occurs more frequently at rest or during exercise in these patients. The aim of the study was to investigate the demographics and circumstances of SCD in a large cohort of HCM patients.

Design: Between 1994 and 2014, 184 consecutive cases of HCM patients who died suddenly (mean age 39±17 years, 70% males) were referred to our cardiac pathology centre. All subjects underwent detailed post-mortem evaluation including histological analysis by an expert cardiac pathologist. Clinical information was obtained from referring coroners.

Results: Only thirty-seven (20%) patients had an established ante-mortem diagnosis of HCM. Forty (22%) patients exhibited cardiac symptoms (16 palpitations, 11 dyspnoea, 7 syncope and 6 chest pain). Maximal wall thickness was 21.4±6.1 mm with a mean heart weight of 548 ± 197 g. Left ventricular (LV) fibrosis was present in 109 patients (59%). Twenty (11%) patients were recreational or competitive athletes (> 3 hours per week of exercise). Thirty-five patients (19%) died during exertion. Of the 149 patients died at rest, 22 (12%) died during sleep. At multivariate analysis, the predictors of death during exertion were age (for older age HR 0.94 (0.92 to 0.97), p<0.001) and gender (for male gender 3.47 (1.04 to 10.19), p=0.03).

Conclusions: Sudden death victims with a diagnosis of HCM were often male, asymptomatic and lacked a diagnosis during life. Sudden death occurred relatively rarely during sport activity. Young age and male gender were the main predictors of death during exercise.

327 Incidence of Psychiatric Illnesses in Sudden Cardiac Deaths

Joseph Westaby, Chandroth Navin Pankajakshan, Mary N Sheppard. St George's University of London, London, United Kingdom.

Background: A retrospective study of the incidence of psychiatric illnesses among 1613 sudden cardiac death cases referred to the Cardiac Risk in Young Cardiovascular Pathology Unit at St. Georges' University of London between 2013-2016. A total of 170 (10.4%) cases with a psychiatric history were found.

Design: The frequency of cases with psychiatric history increased from 13 in 2013, to 56 cases in 2014 and 93 cases in 2015.

Results: The majority were males (61%). Highest incidence was found in 30-39 year group (31%). The mean age was 40 years, the median age was 38 years and the mode for age was 35 years. Psychiatric illnesses reported, depression (47%), non-specified (19%), schizophrenia (11%), anxiety (7%), learning difficulties (6%), psychoses (2%) and others (8%). 95% died either at rest or sleep, 4% died during stress including 4 in police custody. Use of psychiatric medication was reported in 47%. Non-toxic levels of drugs were found in 24.7% of cases, alcohol in 30%.

The commonest cause of death was sudden adult death syndrome with morphologically normal heart (68%), followed by idiopathic left ventricular hypertrophy (8%), cardiomyopathies (8%), ischaemic heart disease (6%), valvular heart disease (2%), hypertensive heart disease (2%) and other causes (6%).

Conclusions: There is disproportionate number of sudden cardiac deaths with psychiatric illnesses and the role of stress and drugs which may effect the electrical activity of the heart must be considered. Medicolegal issues such as death in police custody are important considerations also. Autopsy with detailed cardiac examination is essential in all these cases.

328 Histopathologic and Immunohistochemical Features of Cardiac Myxoma: Review of 28 Cases at a Cardiac Center in Eight Years

Ya Xu, Bettye Cox, Mary R Schwartz, Alberto Ayala, Jae Ro. Baylor College of Medicine, Houston, TX; Houston Methodist Hospital, Houston, TX.

Background: Cardiac myxoma may exhibit focal increased cellularity and lymphoplasmacytic infiltration. The purpose of this study was to analyze the histopathologic features of cardiac myxoma, and to explore the significance of increased cellularity and lymphoplasmacytic infiltration using S-100 and IgG4 immunohistochemical stains.

Design: 28 cases of cardiac myxoma were seen over an 8-year period at an academic tertiary referral hospital with a cardiac center. All the cases were reviewed for clinical and histopathological features. Immunohistochemical stains for calretinin, S-100 protein and Ki-67 were performed on 25 cases with paraffin blocks available, and IgG4 on 13 cases with focal intense lymphoplasmacytic infiltrates.

Results: The age of 28 patients ranged between 24 and 83 years; 20 were women and eight men. The average tumor size was 4.4 cm (range 2.0-10.0 cm) with the largest tumor in the right ventricle. 25 tumors were located in the left atrium. All of the tumors had characteristic stellate cells in a myxoid background. 11 cases had focal increased cellularity, and 13 had focal intense lymphoplasmacytic infiltrates. A unique histologic feature of a palisading growth pattern was seen in 9 of the 11 cases with increased cellularity. No atypia and only rare mitotic activity (<1/10HPFs) was found. Calretinin was strongly positive in all 25 cases. S-100 was expressed in the cellular areas of 9 cases, most prominently in the tumor cells arranged in a palisading pattern. No S-100 expression was identified in the remainder of the cases. None of the cases had increased Ki-67 proliferative fractions (Ki-67 <5% in all cases). Increased IgG4 expression (> 50% plasma cells stained with IgG4) was seen in 2 of 13 cases with focal intense lymphoplasmacytic infiltrates.

Conclusions: Although increased cellularity was seen in 39% of tumors, no increased Ki-67 proliferative fraction was found. Increased IgG4 positive plasma cells were seen in rare cardiac myxomas with focal intense lymphoplasmacytic infiltrates. The significance of increased cellularity with S-100 expression and increased IgG4 expression in tumor pathogenesis, prognosis and therapy remains unclear. Our findings may provide insight for further research work on cardiac myxoma.

Cytopathology

329 Pancreatic Surgical Resections with False-Positive Cytology Results: A Ten-Year Single Institution Retrospective Review

Daniel W Abbott, Bryan Hunt, Tamar Giorgadze, Kiyoko Oshima. Medical College of Wisconsin, Milwaukee, WI.

Background: Pancreatic cytology (PC), including fine needle aspiration (FNA), is an important tool used for the diagnosis of pancreatic lesions and subsequent treatment decisions. This study evaluates the accuracy of PC at a single institution and investigates cases with false positive (FP) malignant PC diagnoses.

Design: 726 pancreas surgical resections (SR) at a single institution received between 2006-2016 were retrospectively reviewed, including 425 SR with corresponding PC. PC was compared to SR results and classified based on agreement of the diagnoses. Slides from SR cases with FP PC diagnoses were reviewed by two cytopathologists in a blinded manner.

Results: The cases selected for analysis included 227 (53.4%) men and 218 (51.3%) women with a mean age of 64.4 years. The corresponding PC cases included 355 (83.7%) pancreatic FNA, 41 (9.7%) bile duct brushings, 18 (4.2%) combined FNA and bile duct brushings, and 31 (7.3%) cases with an unspecified procedure. PC diagnoses included 322 (75.9%) malignant, 18 (4.2%) suspicious for malignancy, 35 (8.3%) atypical, 35 (8.3%) benign, and 14 (3.3%) with another type of diagnosis. PC results agreed with subsequent SR results in 362 (85.4%) cases. False negative PC results were seen in 46 cases (10.8%) and FP PC results were seen in 11 (2.6%) cases. FP cases included 8 (1.9%) cases with documented complete response to neoadjuvant therapy, leaving 3 (0.7%) PC cases that were true FP and are summarized below:

Age/ Sex	PC diagnosis (procedure)	SR diagnosis	Radiology	Elevated markers	Agree/Disagree with original diagnosis
84/F	Malignant, adenocarcinoma (bile duct brush)	Ductal hyperplasia, cholangitis	Common bile duct filling defect, stone vs. neoplasm	CA19.9	1 Agree 1 Disagree
59/F	Suspicious for malignancy, carcinoma (FNA)	Benign mucinous cystic neoplasm	C/W pancreatic pseudocyst	None	2 Disagree
80/F	Malignant, favor endocrine neoplasm	Lymphoplasmacytic sclerosing pancreatitis	Common bile duct mass, favor cholangiocarcinoma	CA19.9 CA125	2 Disagree

Conclusions: FP cytology results were uncommon, with the majority accounted for by complete response following chemotherapy. The discrepancy was resolved in 2 of the 3 cases in which both reviewing cytopathologists agreed that the prior PC result was